Role of electron-electron and electron-phonon interaction effects in the optical conductivity of VO_2

K. Okazaki,[1] S. Sugai,[1] Y. Muraoka,[2] and Z. Hiroi[2]
[1]*Department of Physics, Nagoya University, Nagoya 464-8602, Japan*
[2]*Institute for Solid State Physics, University of Tokyo, Kashiwa 277-8581, Japan*
(Received 2 December 2005; revised manuscript received 24 February 2006; published 17 April 2006)

We have investigated the charge dynamics of VO_2 by optical reflectivity measurements. Optical conductivity clearly shows a metal-insulator transition. In the metallic phase, a broad Drude-like structure is observed. On the other hand, in the insulating phase, a broad peak structure around 1.3 eV is observed. It is found that this broad structure observed in the insulating phase shows a temperature dependence. We attribute this to the electron-phonon interaction as in the photoemission spectra.

DOI: 10.1103/PhysRevB.73.165116 PACS number(s): 71.30.+h, 71.20.Ps, 71.38.−k, 79.60.−i

I. INTRODUCTION

The metal-insulator transition (MIT) is one of the most interesting phenomena in the strongly correlated electron systems.[1] VO_2 is well known for its first-order metal-insulator transition at 340 K,[2] which is accompanied by a structural transition. In the high temperature metallic phase it has a rutile structure, while in the low temperature insulating phase (M_1 phase) the V atoms dimerize along the c axis and the dimers twist, resulting in a monoclinic structure. The magnetic susceptibility changes from paramagnetic to nonmagnetic in going from the metallic to the insulating phase. Hence, this transition is analogous to a Peierls transition. In the early stages of the study for the MIT in VO_2, Goodenough explained the MIT based on a simplified band model.[3] The V $3d$ t_{2g} level is split into the $d_\parallel$ and π^* sublevels due to the tetragonal crystal field. The π^* bands are hybridized with the O $2p\pi$ bands and are pushed upward. The $d_\parallel$ band is rather weakly hybridized with the O $2p$ band and has the lowest energy among the V $3d$ bands. In the metallic phase, the π^* and $d_\parallel$ bands overlap and are partially filled. In the insulating phase, the π^* bands are shifted upward and the $d_\parallel$ band is split into two subbands. As a result, the π^* bands become empty and the lower $d_\parallel$ subband is completely filled.[4] However, this picture was criticized that only with the lattice distortion the optical gap of 0.6 eV (Ref. 5) cannot be reproduced and the importance of electron correlation effects was pointed out based on the cluster calculations.[6] Zylbersztejn and Mott claimed that while the insulating phase cannot be described correctly without taking into account of the electron correlation effect, for the metallic phase of VO_2, the screening effect of the π^* bands on the $d_\parallel$ bands is important.[7]

On the basis of the local-density approximation band-structure calculation, Wentzcovitch *et al.*[8] concluded that the insulating phase of VO_2 is an ordinary band (Peierls) insulator. On the other hand, Cr-doped VO_2 or pure VO_2 under uniaxial pressure in the [110] direction of the rutile structure has another monoclinic insulating phase called the M_2 phase. In the M_2 phase, half of the V atoms form pairs and the other half form zigzag chains.[9] While the V atoms in the pairs are nonmagnetic, those in the zigzag chains have local moments and are regarded as one-dimensional Heisenberg chains according to a NMR study.[10] Based on these observations for the M_2 phase, Rice *et al.*[11] objected to the work of Wentzcovitch *et al.* that the M_2 phase is a Mott-Hubbard insulator and the M_1 phase also must be classified as a Mott-Hubbard insulator. More recently, several theoretical studies have been reported for the MIT of VO_2.[12–15] However, it still remains highly controversial whether the MIT of VO_2 is driven by the electron-phonon interaction (resulting in a Peierls insulator) or the electron-electron interaction (resulting in a Mott insulator).

To address this issue, both of the electron-electron and electron-phonon interaction effects should be further investigated. In a recent photoemission study, it is concluded that while the electron-electron interaction is necessary to produce the band gap in the insulating phase, the electron-phonon interaction is important to fully understand the electronic structure and charge transport in VO_2.[16] To further understand how these effects are related to the charge transport, it is important to investigate the detailed charge dynamics of VO_2. So far, several optical measurements have been reported for VO_2 using bulk samples[5,17,18] and thin film samples.[18,19] However, spectroscopic measurements are difficult for the metallic phase of VO_2 with the bulk crystals because the crystals break into pieces when they cross the MIT.[20] On the other hand, with the thin films, it is difficult to deduce the optical constants precisely from optical measurements because multiple reflections between the film and the substrate should be taken into account.

In this work, we report the optical conductivity of VO_2 at various temperatures deduced from the optical reflectivity measurements of TiO_2 substrates and VO_2 thin films grown on the TiO_2 substrate. It is observed that a broad Drude-like component in the metallic phase transfers to the higher energies around 1.3 eV in the insulating phase. We have also found that the structure around 1.3 eV in the insulating phase shows a temperature dependence similar to the photoemission spectra and we considered that this is another evidence for the strong electron-phonon interaction.

II. EXPERIMENT

VO_2 thin films were epitaxially grown on TiO_2(001) surfaces using the pulsed laser deposition technique as de-

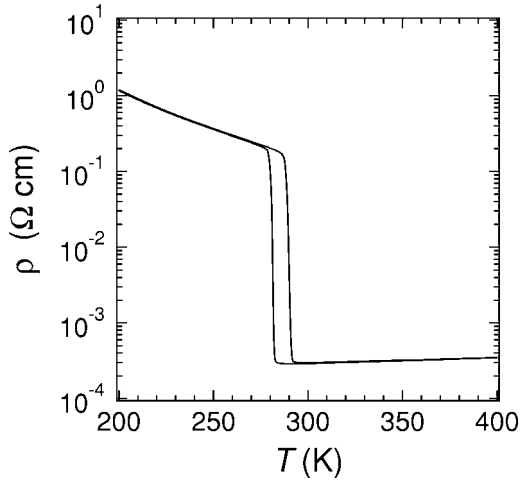

FIG. 1. Electrical resistivity ρ of the VO_2/TiO_2 (001) thin film. A jump of about three orders of magnitude has been observed around 290 K.

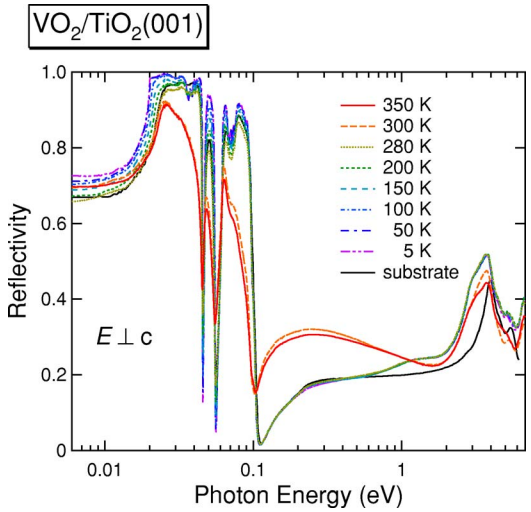

FIG. 2. (Color online) Reflectivity spectra of VO_2/TiO_2 (001) thin films at various temperatures and TiO_2 substrates at 300 K. Below 0.1 eV, because the reflectivity of the substrate is large due to optical phonons, there is an interference effect between the reflection at the substrate and the film.

scribed in Ref. 21. The film thickness was ~100 Å, estimated by four-cycle x-ray diffraction measurements and the MIT was confirmed by electrical resistivity measurements (Fig. 1), showing a jump of about three orders of magnitude around 290 K ($\equiv T_{MI}$). This reduced MIT temperature of the films is due to the compressive strain from the TiO_2 substrate.[21]

Near-normal incidence optical reflectivity measurements were performed using a Fourier-type interferometer (0.006–1.2 eV) and a grating spectrometer (0.8–6.8 eV) from 5 to 350 K. Because VO_2 films have been epitaxially grown on the TiO_2 (001) surface, polarization of the incident light is perpendicular to the c axis of the Rutile structure ($\boldsymbol{E} \perp c$). As a reference mirror, we used an evaporated Au film for the infrared regions and Ag film for the visible region. The experimental error of the reflectivity is less than 0.5% for the far- and near-IR regions and less than 1.0% for the mid-IR, visible, and ultraviolet regions. A detailed procedure to deduce optical constants of VO_2 from the reflectivity is described below.

The normal incidence complex reflectivity of the two layer system can be written as

$$\hat{r}(\omega) = \sqrt{R(\omega)}e^{i\Theta(\omega)}$$

$$= \frac{\hat{r}_{0f} + \hat{r}_{fs}e^{2i\delta_f} + \hat{r}_{0f}\hat{r}_{fs}\hat{r}_{s0}e^{2i\delta_s} + \hat{r}_{s0}e^{2i(\delta_f+\delta_s)}}{1 + \hat{r}_{0f}\hat{r}_{fs}e^{2i\delta_f} + \hat{r}_{fs}\hat{r}_{s0}e^{2i\delta_s} + \hat{r}_{0f}\hat{r}_{s0}e^{2i(\delta_f+\delta_s)}}, \quad (1)$$

where

$$\hat{r}_{0f} = [(n_f + ik_f) - 1]/[(n_f + ik_f) + 1],$$

$$\hat{r}_{fs} = [(n_s + ik_s) - (n_f + ik_f)]/[(n_s + ik_s) + (n_f + ik_f)],$$

$$\hat{r}_{s0} = [1 - (n_s + ik_s)]/[1 + (n_f + ik_f)],$$

$$\delta_f = 2\pi i(n_f + ik_f)d_f/\lambda,$$

and

$$\delta_s = 2\pi i(n_s + ik_s)d_s/\lambda.$$

n_f, k_f, d_f, n_s, k_s, and d_s are the refractive index, the extinction coefficient, and the film thickness of the film and the substrate, respectively, and λ is the wavelength of the incident light.

First, we have measured the reflectivity of the TiO_2 substrates at various temperatures, and then obtained optical constants n_s and k_s using Kramers-Kronig (KK) transformation. For the extrapolation to perform KK transformation, we have assumed a constant value below 0.006 eV and a power-law behavior ($\propto \omega^{-\alpha}, 0 < \alpha < 4$) above 6.8 eV. The value of α was adjusted so that the obtained optical constants reproduced the reported values[22] at 300 K.[23] Next, we have measured the reflectivity $R(\omega)$ of the VO_2/TiO_2 thin films as shown in Fig. 2 and deduced the phase shift $\Theta(\omega)$ using the KK transformation. We have adopted a same assumption with the TiO_2 substrate for the extrapolation. At last, we have obtained the optical constants n_f and k_f by numerically solving the equations obtained from the real and imaginary parts of Eq. (1) multiplied by the denominator on the right-hand side. When solving the equations, we have neglected the terms proportional to $\sin(2\pi n_s d_s/\lambda)$ and $\cos(2\pi n_s d_s/\lambda)$. Because the substrate thickness $d_s \sim 0.5$ mm is much larger than the wavelength λ and is not uniform in the scale of λ, these terms can be replaced with their mean value zero.[24]

III. RESULTS AND DISCUSSION

Figure 3 shows the optical conductivity spectra of VO_2 at various temperatures. The MIT is clearly observed as a spectral weight transfer of the broad Drude-like structure above T_{MI} to the Gaussian-like peak structure around 1.3 eV below T_{MI}. The structure around 1.3 eV can be assigned as a Mott-Hubbard excitation, while an intense peak around 3.8 eV, which is observed both above and below T_{MI}, can be as-

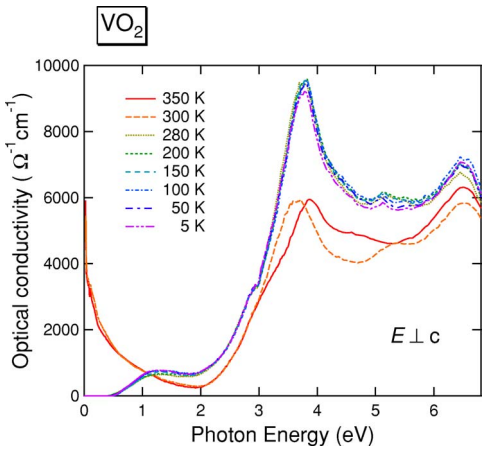

FIG. 3. (Color online) Optical conductivity spectra of VO_2 at various temperatures deduced from the reflectivity spectra of $VO_2/TiO_2(001)$ thin films.

signed as a charge-transfer excitation.[25] In the metallic phase, the value of the optical conductivity in the low-energy region is roughly in accordance with the dc conductivity ($\sim$3500 Ω^{-1} cm^{-1} at 300 K).

In Fig. 4, the number of the effective carriers $[N_{\mathrm{eff}}(\omega)]$ defined as

$$N_{eff}(\omega) \equiv \frac{2m_0V}{\pi e^2}\int_0^{\omega}\sigma(\omega')d\omega' \tag{2}$$

is shown, where m_0 is the bare electron mass and V is the cell volume of the one formula unit. From N_{eff}, the spectral weight of the Drude-like component at 300 K can be estimated as 0.23 per formula unit. From this value, the plasma frequency ω_p and the effective mass m^* can be estimated using a so-called f-sum rule,

$$\int_0^{\omega_0}\sigma(\omega)d\omega = \tfrac{1}{8}\omega_p^2, \tag{3}$$

where ω_p is defined as $\omega_p^2 = 4\pi ne^2/m^*$, ω_0 is taken as the energy for the upper limit of the contribution of the Drude-like component (=2.0 eV), and n is the charge density (=1/V

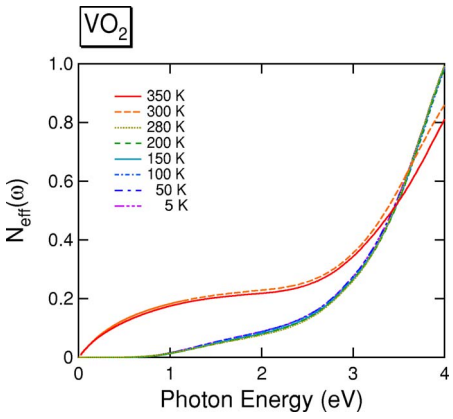

FIG. 4. (Color online) Effective carrier number per formula unit N_{eff} of VO_2 obtained by integrating the optical conductivity.

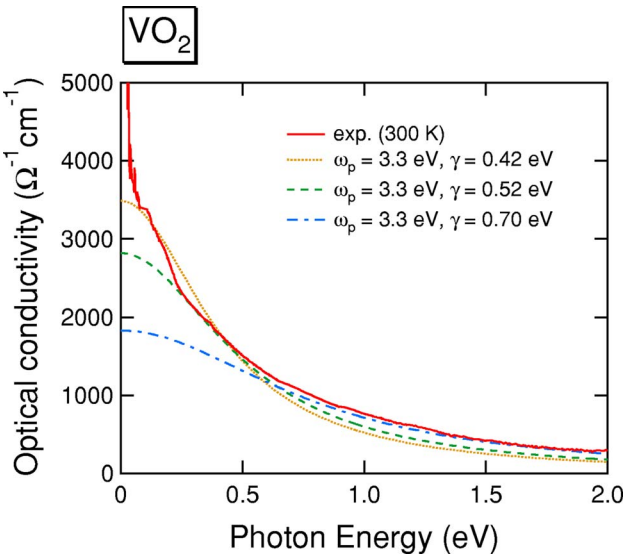

FIG. 5. (Color online) Comparison of the optical conductivity of VO_2 in the metallic phase with the simple Drude model.

i.e., one electron per formula unit). Thus, ω_p and m^*/m are estimated as 3.3 eV and 4.3, respectively. These values agree well with those estimated from the peak position of the energy-loss function $\mathrm{Im}(-1/\epsilon(\omega))$ by assuming its peak position corresponding to $\omega_p/\sqrt{(\epsilon_\infty)}$,[26] where ϵ_∞ is the optical dielectric constant and estimated as $\sim$8 from $\mathrm{Re}(\epsilon(\omega))$ at ω=2.0 eV. The spectra of $\mathrm{Im}(-1/\epsilon(\omega))$ at 300 K has a peak at 1.15 eV and the ω_p is estimated as 3.25 eV. From this consistency, we can say that the obtained mass enhancement factor m^*/m_0 should be a reasonable one. For another vanadium oxide d^1 system $Sr_{1-x}Ca_xVO_3$, which is metallic at all temperatures, m^*/m_0 has been estimated as $\sim$3.1 for $CaVO_3$ and $\sim$2.7 for $SrVO_3$ from optical measurements.[27] Hence, m^*/m_0 of VO_2 is somewhat larger than that of $Sr_{1-x}Ca_xVO_3$. Hence, we can say that the quasiparticle renormalization or the electron correlation effect in VO_2 is stronger than $Sr_{1-x}Ca_xVO_3$. This is consistent with the quasiparticle renormalization factor Z estimated from photoemission spectroscopy. They have been estimated as $\sim$0.3 for VO_2 (Ref. 16) and $\sim$0.5 for $Sr_{1-x}Ca_xVO_3$ (Ref. 29), respectively.

Using the value of ω_p estimated above, we have compared the optical conductivity at 300 K with the simple Drude model with various γ (scattering rate) in Fig. 5. In the simple Drude model, the optical conductivity is given by $\sigma(\omega) = \omega_p^2\gamma/4\pi(\omega^2+\gamma^2)$. With a larger value of γ, the simple Drude model seems to fit in the higher-energy region. However, it cannot reproduce the whole line shape of the optical conductivity with the only one value. This should correspond to the energy dependence of the γ. Then, we introduce the energy dependence in γ and m^*/m_0 using the extended Drude model according to Ref. 27. Figure 6 shows $\gamma(\omega)$ and $m^*(\omega)/m_0$ at 300 K above 0.1 eV. As expected from the comparison with the simple Drude model, $\gamma(\omega)$ increases with the photon energy and is almost proportional to ω, while the energy dependence of $m^*(\omega)/m$ is not so large. A similar behavior has been observed in other transition-metal oxides.[27,30] However, it seems to be a still open question why

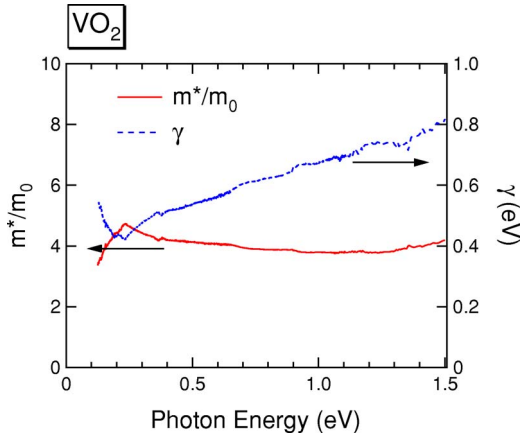

FIG. 6. (Color online) Energy-dependent mass enhancement factor $m^*(\omega)/m_0$ and the scattering rate $\gamma(\omega)$ deduced from the extended Drude model.

$\gamma(\omega)$ is proportional to ω rather than ω^2 as expected from the standard Fermi liquid theory.

Although the behavior of $\gamma(\omega) \propto \omega$ is commonly observed in other transition-metal oxides, the value of $\gamma(\omega)$ of VO_2 is somewhat larger compared to $Sr_{1-x}Cr_xVO_3$. For the case of VO_2, this feature may related to the temperature dependence of the electronic resistivity. Allen *et al.*[31] have reported that the resistivity of the single crystal VO_2 shows a linear temperature dependence and does not saturate at least up to 840 K. They have estimated the mean free path ~3 Å at 800 K and claimed that VO_2 might not be a conventional Fermi liquid. When the mean free path is such small, a description for the electronic transport by the Boltzmann equation may be not valid. However, the unexpected small mean free path is due to the large scattering rate and hence, these features in the electronic resistivity and the optical conductivity may be related to the characteristic scattering mechanism in VO_2.

Next, we would like to discuss the optical conductivity spectra in the insulating phase. Figure 7 shows the optical conductivity spectra of VO_2 in the region of the Mott-Hubbard excitation. The contribution from the higher-energy peak is subtracted by assuming as shown in the inset. We would like to note that the peak position of this excitation is far less than twice of the peak position of V 3*d* peak of the photoemission spectra (~1.0 eV). For example, the dynamical mean field theory predicts that the spectral function of the half-filled Hubbard model has peaks at $\omega=-U/2$ and $U/2$ corresponding the lower- and upper-Hubbard band, respectively, and that the optical conductivity has a peak at $\omega=U$ in the insulating region. In fact, $Sr_{1-x}Ca_xVO_3$ and V_2O_3 have been interpreted within this scheme.[27,28] For the case of VO_2, the different *d*-electron bands, $d_\parallel$ and π^* bands[3] could be related to this transition. Because the polarization of the incident light is $\boldsymbol{E} \perp c$, the occupied $d_\parallel$ orbitals cannot transfer to the nearest-neighbor V atoms along the *c* axis (See Fig. 8). Hence, this structure is assigned to the *d*-*d* transfer to the second-nearest-neighbor V atoms. Furthermore, $d_\parallel$ orbitals between the second-nearest-neighbor V atoms are orthogonal; this structure should be the $d_\parallel$-π^* transition between the second-nearest-neighbor V atoms.

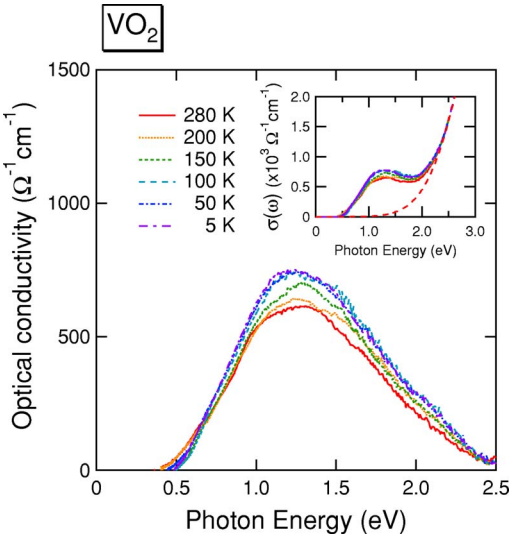

FIG. 7. (Color online) Temperature dependence of the optical conductivity of VO_2 in the insulating phase in the region of the Mott-Hubbard excitation after the subtraction of the contribution from the higher-energy peak.

The spectra in Fig. 7 have the similar line shapes and show a similar temperature dependence to the photoemission spectra. Because the optical conductivity spectra in Fig. 3 show almost no temperature dependence around the region from 2.5 to 3.0 eV in the insulating phase, the same Gaussian function was used to subtract the contribution from the higher-energy peak for all the spectra in Fig. 7. Hence, this subtraction procedure does not affect the temperature dependence below 2.5 eV. In the recent photoemission study,[16] the line shape of the V 3*d* band and its temperature dependence has been reproduced by the independent boson model and is attributed to the strong electron-phonon coupling. Using the independent boson model, the optical conductivity at finite

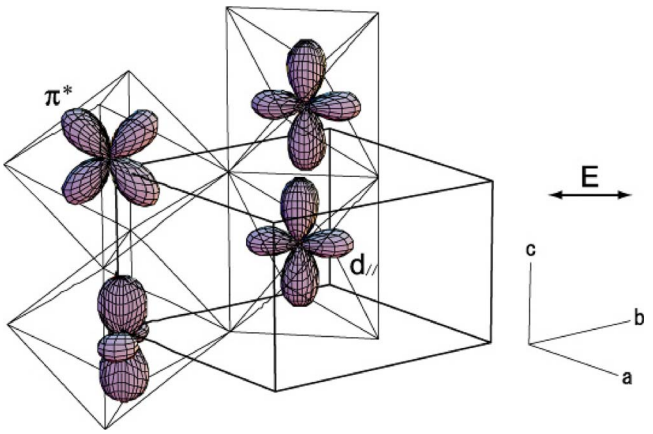

FIG. 8. (Color online) Configuration between the $d_\parallel$ and π^* orbitals. The occupied $d_\parallel$ orbitals can transfer to the unoccupied π^* orbitals of the second-nearest-neighbor V atom with the $\boldsymbol{E} \perp c$ polarization, while it cannot transfer to the $d_\parallel$ orbitals of the nearest- and the second-nearest-neighbor V atoms. Thick lines indicate the unit cell of the rutile structure and thin lines indicate oxygen octahedra. (Note that the unit cell volume in the insulating phase is twice as that of the rutile structure in the metallic phase.)

temperature can be written by a similar expression to the spectral function,[32]

$$\sigma(\omega) \propto \frac{\pi}{\omega} e^{-g_{if}(2N+1)} \sum_l \frac{g_{if}^l}{l!} \sum_{m=0}^{l} {}_lC_m N^m (N+1)^{l-m} \times \delta[\omega - \varepsilon_i + \varepsilon_f + \Delta_i - \Delta_f - (l-2m)\omega_0].$$

This describes a transition from the initial state i to the final state f. N is the phonon occupation number, g_{if} is the effective electron-phonon coupling constant, which is dependent on the electron-phonon coupling of both the initial and final states, ω_0 is the phonon energy, ε_i and ε_f are the energies of the initial and final states, respectively, and Δ_i and Δ_f are the electron self-energies of the initial and final states, respectively. From this expression, similar temperature dependence to the photoemission spectra is expected for the optical conductivity. Hence, we conclude that the temperature dependence of the optical conductivity is another evidence for the strong electron-phonon interaction.

IV. CONCLUSION

We have studied the charge dynamics of VO_2 by the optical reflectivity measurements. The optical conductivity clearly shows a metal-insulator transition. In the metallic phase, the spectral weight of the Drude-like component and the mass enhancement factor m^*/m_0 have been estimated as ~0.23 and 4.3, respectively. This m^*/m_0 is somewhat larger than another d^1 vanadium oxide $Sr_{1-x}Ca_xVO_3$. From this, we have concluded that the electron correlation effect in VO_2 is stronger than $Sr_{1-x}Ca_xVO_3$. From the extended Drude model, $\gamma(\omega)$ is rather large and almost proportional to ω. This would be related to the characteristic scattering mechanism in the metallic phase of VO_2. In the insulating phase, the broad Gaussian-like structure has been observed around 1.3 eV. This would be a $d_{\|}$-π^* transition between the second-nearest-neighbor V atoms. This structure shows a similar temperature dependence to the photoemission spectra. We have concluded that this is another evidence for the strong electron-phonon coupling.

ACKNOWLEDGMENTS

The authors would like to thank J. Matsuno and A. Fujimori for enlightening discussions. This work was partially supported by the 21st Century COE program of Nagoya University and by a Grant-in-Aid for Scientific Research from the Ministry of Education, Culture, Sports, Science and Technology, Japan.

[1] M. Imada, A. Fujimori, and Y. Tokura, Rev. Mod. Phys. **70**, 1039 (1998).
[2] J. Morin, Phys. Rev. Lett. **3**, 34 (1959).
[3] J. B. Goodenough, J. Solid State Chem. **3**, 490 (1971).
[4] See Fig. 3 and Fig. 4 in Ref. 3.
[5] L. Ladd and W. Paul, Solid State Commun. **7**, 425 (1969).
[6] C. Sommers, R. de Groot, D. Kaplan, and A. Zylbersztejn, J. Phys. (France) Lett. **36**, L157 (1975); C. Sommers and S. Doniach, Solid State Commun. **28**, 133 (1978).
[7] A. Zylbersztejn and N. F. Mott, Phys. Rev. B **11**, 4383 (1975).
[8] R. M. Wentzcovitch, W. W. Schulz, and P. B. Allen, Phys. Rev. Lett. **72**, 3389 (1994).
[9] M. Marezio, D. B. McWhan, J. P. Remeika, and P. D. Dernier, Phys. Rev. B **5**, 2541 (1972).
[10] J. P. Pouget, H. Lauois, T. M. Rice, P. Dernier, A. Gossard, G. Villeneuve, and P. Hagenmuller, Phys. Rev. B **10**, 1801 (1974).
[11] T. M. Rice, H. Launois, and J. P. Pouget, Phys. Rev. Lett. **73**, 3042 (1994).
[12] A. Tanaka, J. Phys. Soc. Jpn. **72**, 2433 (2003).
[13] S. Biermann, A. Poteryaev, A. I. Lichtenstein, and A. Georges, Phys. Rev. Lett. **94**, 026404 (2005).
[14] A. Liebsch, H. Ishida, and G. Bihlmayer, Phys. Rev. B **71**, 085109 (2005).
[15] M. S. Laad, L. Craco, and E. Muller-Hartmann, Europhys. Lett. **69**, 984 (2005).
[16] K. Okazaki, H. Wadati, A. Fujimori, M. Onoda, Y. Muraoka, and Z. Hiroi, Phys. Rev. B **69**, 165104 (2004).
[17] A. S. Barker, Jr., H. W. Verleur, and H. J. Guggenheim, Phys. Rev. Lett. **17**, 1286 (1966).
[18] H. W. Verleur, A. S. Barker, Jr., and C. N. Berglund, Phys. Rev. **172**, 788 (1968).
[19] H. S. Choi, J. S. Ahn, J. H. Jung, T. W. Noh, and D. H. Kim, Phys. Rev. B **54**, 4621 (1996).
[20] K. Okazaki, A. Fujimori, and M. Onoda, J. Phys. Soc. Jpn. **71**, 822 (2002).
[21] Y. Muraoka and Z. Hiroi, Appl. Phys. Lett. **80**, 583 (2002).
[22] M. W. Ribarsky, in *Handbook of Optical Constants of Solids*, edited by E. D. Palik (Academic Press, Orlando, 1985).
[23] F. Woooten, *Optical Properties of Solids* (Academic Press, New York, 1972).
[24] P.-O. Nilsson, Appl. Opt. **7**, 435 (1968).
[25] T. Arima, Y. Tokura, and J. B. Torrance, Phys. Rev. B **48**, 17006 (1993).
[26] Strictly, even in the simple Drude model, only when γ is small enough, the peak position of the energy-loss function is located at $\omega_p/\sqrt{(\epsilon_\infty)}$.
[27] H. Makino, I. H. Inoue, M. J. Rozenberg, I. Hase, Y. Aiura, and S. Onari, Phys. Rev. B **58**, 4384 (1998).
[28] M. J. Rozenberg, G. Kotliar, H. Kajueter, G. A. Thomas, D. H. Rapkine, J. M. Honig, and P. Metcalf, Phys. Rev. Lett. **75**, 105 (1995).
[29] A. Sekiyama, H. Fujiwara, S. Imada, S. Suga, H. Eisaki, S. I. Uchida, K. Takegahara, H. Harima, Y. Saitoh, I. A. Nekrasov, G. Keller, D. E. Kondakov, A. V. Kozhevnikov, Th. Pruschke, K. Held, D. Vollhardt, and V. I. Anisimov, Phys. Rev. Lett. **93**, 156402 (2004).
[30] T. Katsufuji, Y. Okimoto, T. Arima, Y. Tokura, and J. B. Torrance, Phys. Rev. B **51**, 4830 (1995).
[31] P. B. Allen, R. M. Wentzcovitch, W. W. Schulz, and P. C. Canfield, Phys. Rev. B **48**, 4359 (1993).
[32] G. D. Mahan, *Many-Particle Physics* (Plenum, New York, 1981), Sec. 4.3.